Kinetic Evidence of the Maillard Reaction in Hydrothermal Biomass Processing: Glucose−Glycine Interactions in High-Temperature, High-Pressure Water

Andrew A. Peterson,[†] Russell P. Lachance,[‡] and Jefferson W. Tester[§,*]

Department of Chemical Engineering, Massachusetts Institute of Technology, Cambridge, MA

Kinetic and mechanistic evidence is presented of the occurrence of a Maillard-type reaction under conditions of interest to hydrothermal biomass processing. Glucose−glycine mixtures were reacted at 250 °C and 10 MPa in an excess of water; both glucose and glycine were found to strongly influence the destruction kinetics of the other species and to result in quantitative and qualitative changes, such as strong absorbance at 420 nm and the production of a dark brown appearance and nutty odor, which are characteristic of the Maillard reaction. The presence of glucose always resulted in higher glycine destruction; the presence of glycine resulted in increased or decreased glucose destruction, depending on initial concentrations, which is consistent with results reported in the literature for lower temperature Maillard reactions. Surrogate compounds that contain the same chemical functional groups also resulted in similar trends. As a result of this reaction, the presence of proteins and amino acids in biomass feedstocks can be expected to result in processing difficulties at hydrothermal conditions: these difficulties will include fouling of process equipment, the quenching of desired reaction pathways, and difficulty in achieving separations between aqueous and oil phases produced.

1. Introduction

Hydrothermal technologies have the potential to produce conventional fuels with high efficiency from a variety of biomass feedstocks, including waste products.[1] Among the advantages of using hydrothermal processing methods in the conversion of biomass into fuels is the ability of these processes to use a variety of mixed feedstocks. For instance, the Paul Scherrer Institut has demonstrated its supercritical water gasification process on wood sawdust as well as on swine manure, with high yields of methane in each case.[2−4] Elliott et al.[5] have demonstrated the gasification of distiller's grains, a byproduct of ethanol production, as well as several other feedstocks in their process being developed at Pacific Northwest National Laboratory. Researchers in The Netherlands have demonstrated liquefaction of a range of feedstocks, including sugar beet pulp, into a reduced-oxygen "bio-crude".[6] And finally, Changing World Technologies operates a 200 ton/day commercial plant that converts turkey offal into fuel oils.[7,8]

While hydrothermal technologies have been shown to handle a range of feedstock compositions, in actuality, the processes are susceptible to the individual makeup of the feedstocks and must be tailored to the chemistry taking place as a result of the feedstock composition and processing conditions. The most well-known example of this is the effect that salts present in feedstocks can have on the processing conditions required in near- and supercritical water.[9−12]

Empirical evidence indicates that an interaction between proteins and carbohydrates may be causing unexpected results with certain biomass feedstocks; these interactions have characteristics similar to the Maillard reaction, which is caused by a reaction of the amine group present in proteins with the carbonyl group present in carbohydrates. The Maillard reaction has been extensively studied over the course of several decades and is reported in a broad range of food, agricultural, and medical literature, but in conditions that are generally limited to those encountered in food processing, usually at temperatures less than 150 °C or in dry heat. Figure 1 shows an overview of the Maillard reaction network, in a similar form to that mapped out by Hodge in 1953.[13] The first step of the reaction takes place when the lone pair of electrons on the primary amine group of the amino acid undertakes a nucleophilic attack onto the carbonyl group of the sugar. This reaction network is shown with glucose and glycine as example starting reactants, but of course any reducing sugar and amino acid could also follow a similar reaction mechanism. The sugar and amino acid combine to form the so-called Amadori compound, then, in the second stage of the Maillard reaction, the Amadori compound undergoes a number of reactions, the products of which include fission products and large polymeric materials, which are broadly referred to as melanoidins. The Maillard reaction is clearly not a single reaction pathway, but is an interconnected reaction network; see the work of Martins[14] for a recent overview of the Maillard reaction pathways and kinetics as known at moderate temperatures. The products of the Maillard reaction are responsible for many of the characteristic brown colors and flavors in food, including the brown color of bread crust, many of the flavors of grilled meat, the colors associated with beer (imparted during the roasting of the malted barley), and the brown colors and flavors associated with most baked goods. The Maillard reaction can also occur in the body and has more recently attracted significant attention in the medical literature, where it is often referred to as glycation. Here, Maillard end products have been associated with a number of age-related diseases, including diabetes, Alzheimer's disease, and cancer, although considerable uncertainty exists as to whether these chemicals are a cause of or are simply correlated with these conditions.[15]

Changing World Technologies, Inc., (CWT) operates a commercial processing facility that produces fuel oil by hydrothermally converting and separating waste products associated with the processing of turkey. In their process, turkey offal, a

* To whom correspondence should be addressed. E-mail: jwt54@cornell.edu. Phone: 1-607-254-7211. Fax: 1-607-255-9166.

[†] Currently with the Technical University of Denmark, Lyngby, Denmark.

[‡] Currently with the United States Military Academy, West Point, NY.

[§] Currently with Cornell University, Ithaca, NY.

10.1021/ie9014809
Published on Web 01/28/2010

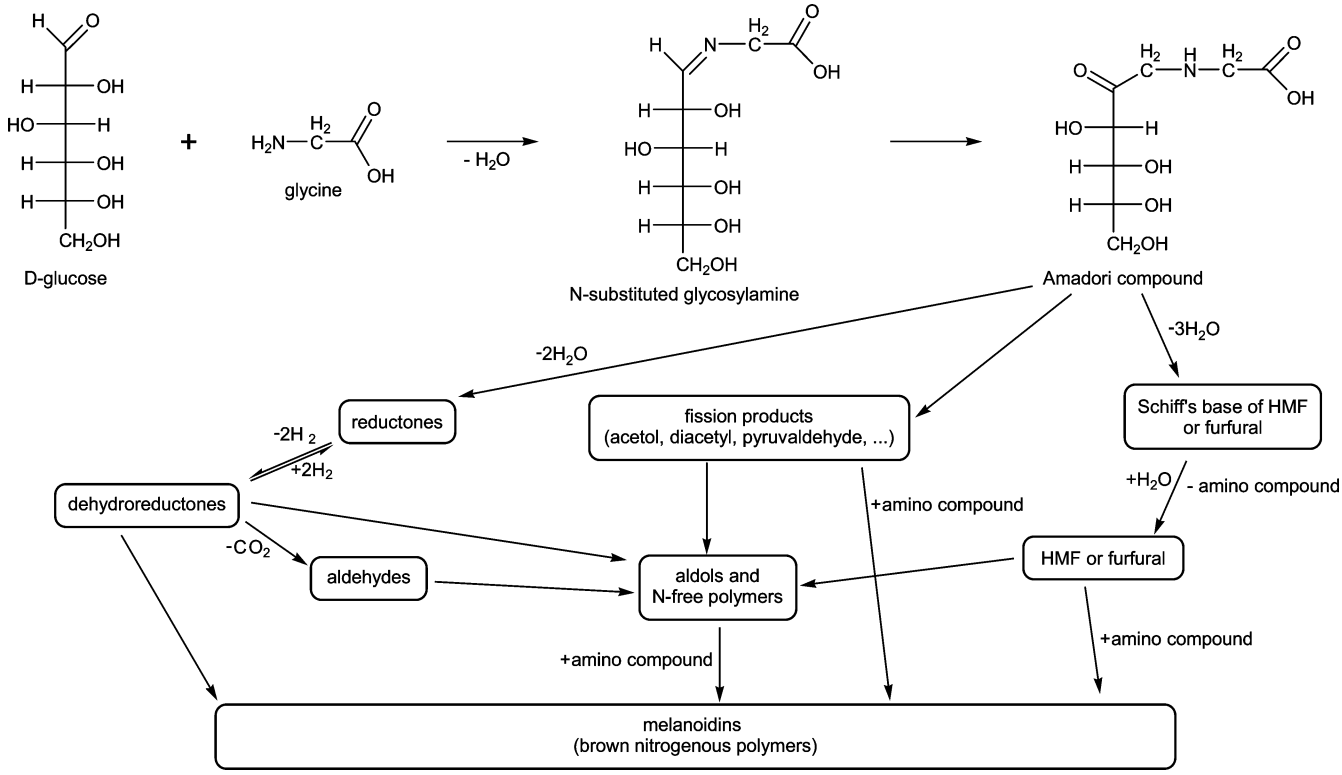

Figure 1. Overview of the Maillard reaction network. Adapted from refs 13 and 14.

Figure 2. Undesirable "emulsified" or "polymerized" product produced under certain processing conditions. Figure provided by Changing World Technologies, Inc., used with permission.

waste stream which makes up approximately 50% of the weight of the turkey entering a turkey processing plant, is thermally processed at 250 °C and at pressure higher than the vapor pressure of water, in order that processing is done in the presence of liquid water.[1,7] The CWT process is designed to have a phase split between the fuel (oil) phase and the aqueous phase at the end of their hydrothermal process. However, under certain conditions, a brown, inseparable emulsified product is produced instead.[16] A picture of this product is shown in Figure 2. This product is of high viscosity and makes the separation of the two phases impractical. CWT found that they could suppress this phenomenon by the addition of sulfuric acid but did not isolate the cause of the problem.

Several factors suggest that a Maillard-type reaction may have caused the phenomenon observed by CWT. The CWT feedstock is meat processing waste that would contain significant quantities of the proteins and sugars needed for the Maillard reaction. The colors and high viscosities observed are consistent with Maillard reaction products. Also, at lower temperatures, the Maillard reaction is known to be suppressed by low pH, consistent with the solution employed by CWT.

Separately, Kruse et al.[17] at the Forschungszentrum Karlsruhe studied the gasification of biomass at 500 °C and 30 MPa. They found that when zoomass (actually chicken/rice baby food, due to the ease with which it can be pumped) was used as a feedstock, the extent of gasification was significantly lower than when they used phytomass (carrot/potato baby food) or when they used a glucose/K_2CO_3 solution. The researchers speculated that this may have been caused by the relatively high protein content, which was about 47 wt % on a dry basis in the zoomass.

In a follow-up study, Kruse et al.[18] used model compounds to determine if the proteins could be responsible for the suppressed gasification that they observed. They found that when a solution of 2 wt % glucose, with 0.2 wt % $KHCO_3$, was gasified, the addition of alanine had the effect of decreasing the yield of gases, while increasing the CO content of the gas produced; these results were consistent with the results of gasification of the zoomass that they reported earlier. Therefore, they determined that protein/amino acid content interfered with the gasification process and speculated that free radical scavengers produced by the Maillard reaction may have caused the decrease in the gasification.

No studies have directly examined a simple mixture of model amino acids and carbohydrates under hydrothermal conditions in order to determine if a Maillard-type reaction occurs. In the current study, we set out to explore a system of glucose, as a model carbohydrate, and glycine, as a model protein, to search

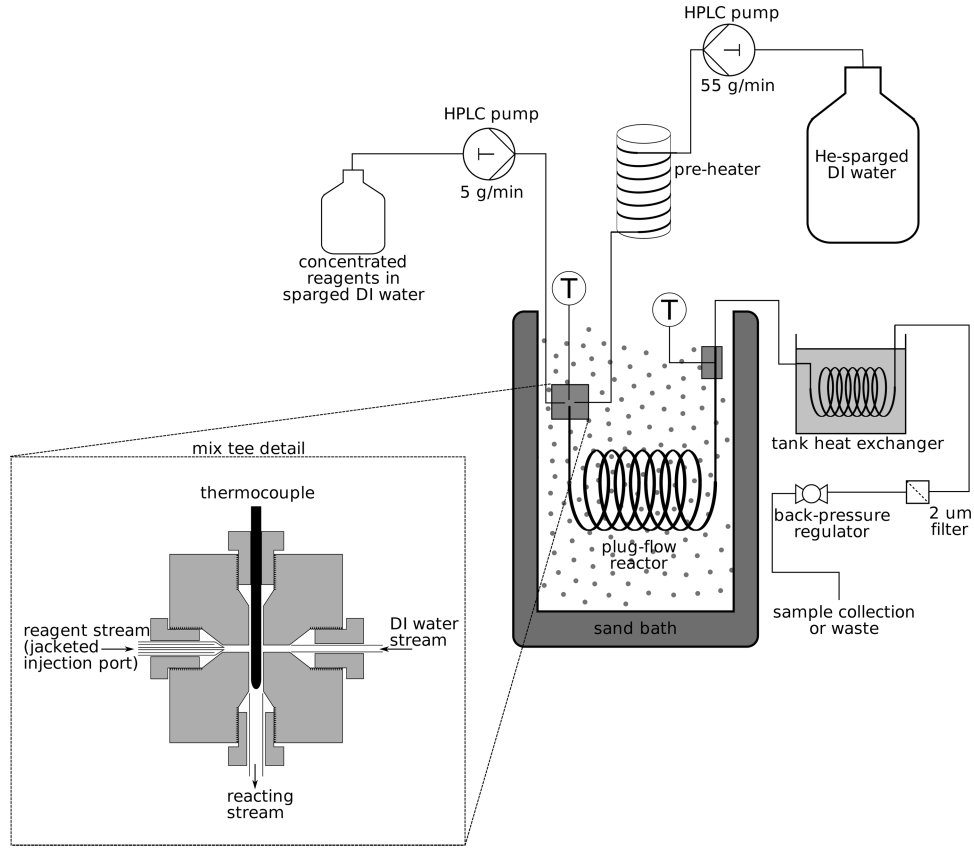

Figure 3. Reactor schematic.

for kinetic and qualitative evidence of a Maillard-type reaction at hydrothermal conditions of 250 °C and 10 MPa.

Related Studies. Inoue, Minowa, and co-workers[19,20] studied the degradation of melanoidins in hydrothermal media. Melanoidins are polymeric products produced by the Maillard reaction. The researchers report using glucose−glycine mixtures to study the decomposition of melanoidins in hydrothermal media in order to understand the origin of nitrogen in oils produced by hydrothermal liquefaction. In their studies, the researchers "gradually" heated glucose−glycine mixtures in water in a 100-mL autoclave until a reaction temperature of 150 to 350 °C was reached, over the course of 12 to 29 min. When the vessel reached the desired temperature of 150 to 350 °C, the vessel was "rapidly cooled". In batch experiments such as these, it is impossible to say under what conditions reactions are taking place; however, it can be presumed that the glucose and glycine had completely reacted at low temperatures. The researchers report that the melanoidins increasingly form water-insoluble oils as the final reaction temperature was raised at the expense of detected melanoidins, which they define as the water-soluble, diethyl-ether-insoluble product fraction. They do not speculate as to where the unreported mass is in their product distribution: presumably it is in the form of chars or gaseous products.

A number of studies have examined the effect of high pressures on the Maillard reaction at processing temperatures of 60−100 °C. These studies were generally motivated by the use of high-pressure processing in the food industry as a means of sterilization. Pressures as high as 600 MPa were studied over these mild temperatures, and the amount of Maillard reaction occurring was found to be affected by the high pressures. Depending on reaction conditions, the extent of reaction could be found to increase or decrease with added pressure.[21−23]

2. Materials and Methods

2.1. Reactor System Overview. In order to examine reactions between model protein and carbohydrate molecules, a continuous plug-flow reactor system was designed to operate isothermally with precisely controlled residence times. A schematic of the reactor system is shown in Figure 3. By mixing a hot water and cold feed stream at specified conditions, the reaction starting time could be precisely specified.

A brief description of the reactor setup follows, but more detailed information on design considerations of the reactor can be found in ref 24. For standard run conditions, a Dynamax SD-1 pump was used to deliver 55 mL/min of deionized water at the reaction pressure of 10 MPa. This water stream entered a preheater in which it was heated well above the reaction temperature (∼280 °C). Separately, a feed stream was prepared that contained the concentrated reactants glucose and glycine. This stream was pumped at 5 g/min by an Acuflow Series II HPLC pump. The cold and hot streams met in a custom-fabricated mixing tee built to specifications by High Pressure Equipment Co (HiP); see Figure 3. The cold stream (containing the reactants) entered the mixing tee through a jacketed injection port to ensure that it was not heated before mixing with the hot stream; cooling water circulates through the port's jacket. A thermocouple extended into the mixing tee to measure the reactor entrance temperature; the narrowing of the passageway caused by the thermocouple may have also aided in the mixing of the two streams.[25]

Two different plug-flow reactors were employed in these experiments. Both reactors were constructed of Inconel 625 (UNS N06625) and consisted of a long, coiled piece of tubing immersed in the sandbath. The majority of the experiments were carried out in the reactor that will be designated "R12", which

was 7.37 m in length and had an internal diameter of 1.0 mm and a measured internal volume of 6.22 ± 0.04 mL. Some reactions were carried out in reactor "R13", which was 11.23 m in length and 1.0 mm in diameter, with a measured internal volume of 9. 54 ± 0.08 mL. Under typical operating conditions, the reactor was calculated to have a residence time of 5.0 to 7.5 s, with an estimated experimental error of ±0.1−0.2 s. The set of experiments that involved glycine alone for residence times on the order of minutes (reported in Figure 6) were conducted in the continuous stirred tank reactor built and described by Marrone.[26]

The reactor and mixing tee were located in an isothermal sandbath (Tescom Fluidized Bath SBS-4) kept at 250 ± 4 °C. Upon exiting the reactor, the hot stream immediately entered a coiled piece of 1/16-in. tubing submerged in a room-temperature water bath to quench the reaction; this quench period was designed to be fast enough to have only a negligible effect on the measured extent of reaction.[24] The flow then passed through a 2-μm inline filter and a back-pressure regulator. Samples were collected after the back-pressure regulator. For each run condition, the system was allowed to stabilize for 45 min, then six independent effluent samples were taken with approximately eight-minute spacing between samples.

Reactions were carried out at 250 °C; this is a temperature sufficiently elevated above the range in which the Maillard reaction is typically studied in aqueous systems, but still at a low enough temperature that meaningful kinetic data could be measured without the complete destruction of the reactants. Typical initial concentrations of glucose and glycine were quite dilute, on the order of 1 to 10 mmolal, in the experiments reported here. All initial concentrations reported are concentrations at the reactor entrance. These concentrations were kept dilute in order to measure the reaction kinetics between the two compounds without producing large amounts of polymeric material, which were found to be produced in high quantities in early screening experiments that were conducted at higher concentrations and in reactors with larger residence times. The polymeric material produced in these earlier experiments had the unfortunate effect of interrupting runs by plugging filters and clogging the back pressure regulator. Therefore, run conditions were focused on the range of 1−10 mmolal of each species with a 5−10 s residence time at 250 °C and 10 MPa, which allowed good observation of the initial kinetics of this reaction without leading to the production of solid/polymeric equipment-clogging precipitates.

2.2. Chemical Reagents and Solution Preparation. Deionized water was produced using an ELGA Purelab Ultra water system to a resistivity of 18.2 MΩ cm. The deionized water was sparged for at least 10 min with ultrahigh purity compressed helium and kept under helium head pressure to ensure oxygen-free conditions.

Glucose (anhydrous, granular) and glycine were purchased from Mallinckrodt Chemicals and mixed into deionized water to form the reagent feed. This feed stream was also sparged and kept under head pressure with helium. The concentrations of all feed solutions were verified by the standard analytical techniques for glycine and glucose as outlined below.

2.3. Analysis of Reactor Effluent. Glycine concentrations were determined with high-pressure liquid chromatography (HPLC) using a 250 × 4.6 mm Alltech Alltima Amino column (5 μm) from Grace-Davison. A mobile phase of 67% (v/v) acetonitrile and 33% water was delivered at 1 mL/min using a Dionex IP25 isocratic pump. The column was kept at 30 °C using a column heater from Timberline Instruments Company. Samples were injected using a Rainin Dynamax AI-200 Automatic Sample Injector with a 20-μL sample loop, and the presence of glycine was detected at 190 nm with a Rainin Dynamax UV-DII Absorbance Detector. Data was acquired to a PC running Dynamax PC Chromatography Workstation version 1.9. The HPLC was recalibrated during each run with samples containing 1, 5, and 10 mmolal glycine.

Glucose is more difficult to detect than glycine using standard HPLC methods due to its lack of absorbance in the UV range. Thus, two different methods were used for detection of glucose at different times in this study. In the bulk of the experiments reported in this paper, glucose was analyzed via a YSI 2700 SELECT Biochemistry Analyzer, which uses immobilized glucose oxidase enzyme between porous polycarbonate and cellulose acetate membranes. The glucose oxidase enzyme selectively oxidizes glucose present in the sample, and the machine measures H_2O_2 production from this enzymatic reaction via a platinum electrode. The resulting current is proportional to glucose concentration in the sample. In later runs carried out for this study, the HPLC method for glycine was made to work for glucose by the addition of an evaporative light-scattering detector (ELSD) to the HPLC system downstream of the UV detector. The ELSD functions by volatilizing the liquid HPLC effluent that passes through it; any dissolved chemicals that are less volatile than the mobile phase can be detected by scattering of a laser beam passing through the volatilized flow. The ELSD provided good sensitivity to glucose and was used in all experiments conducted after its installation. Both methods were recalibrated daily.

Other compounds analyzed for, including glycine anhydride and 5-hydroxymethylfurfural, were analyzed using a separate HPLC employing an organic acid column and a variable-wavelength UV detector. In this system, a 0.01 N sulfuric acid (in water) solution was used as the mobile phase. The mobile phase was degassed using a Waters AF inline degasser and delivered at 0.7 mL/min to the column. The column, an Interaction ORH-801 organic acid column, was kept at 60 °C by a Timberline column heater. The sample loop size used was 20 μL. Compounds were detected either with a UV diode array detector (Beckman Model 168) capable of scanning UV wavelengths or a Dynamax Model UV-1 fixed wavelength detector.

The reactor effluent was also analyzed for absorbance in the UV and visible spectrum by a Cary Model 50 Scan UV-visible spectrophotometer. Absorbance was measured over the range of 1100−190 nm at a scan rate of −300 nm/min with a data interval of 0.5 nm. The absorbance of the reactor effluent was referenced to the absorbance of a pure sample of deionized water. The sample vial path length was 12.5 mm.

3. Results and Discussion

Pure Glucose and Pure Glycine in Water. Glucose is well-known to be quite reactive on its own in hydrothermal media,[1] and this study confirms that behavior. Figure 4 shows the destruction of glucose as a function of the initial glucose concentration, for reaction conditions of 250 °C, 10 MPa, 5.0 s residence time, and with no glycine present. As the glucose concentration increases, the relative amount of glucose destroyed in this 5 s reaction decreases fairly dramatically, from approximately 50% to less than 20% destroyed. This is indicative of reaction kinetics of less than first order. The curve in Figure 4 is the reaction kinetic curve fit assuming that the reaction follows kinetics of the form $r = kC^n$, where C is the glucose concentration, r is the rate of glucose conversion, and k and n

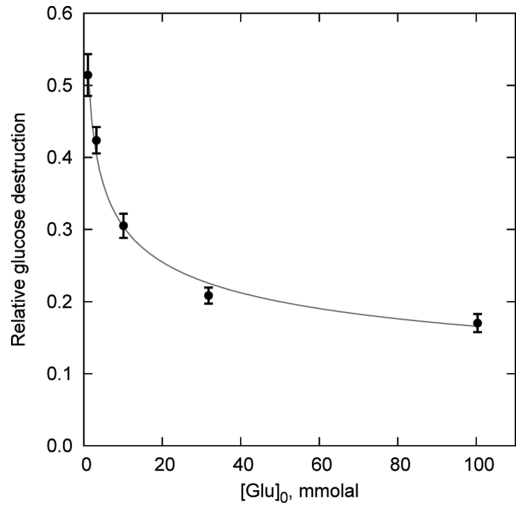

Figure 4. Glucose destruction in the absence of glycine, at 250 °C, 10 MPa, and 5.0 s residence time.

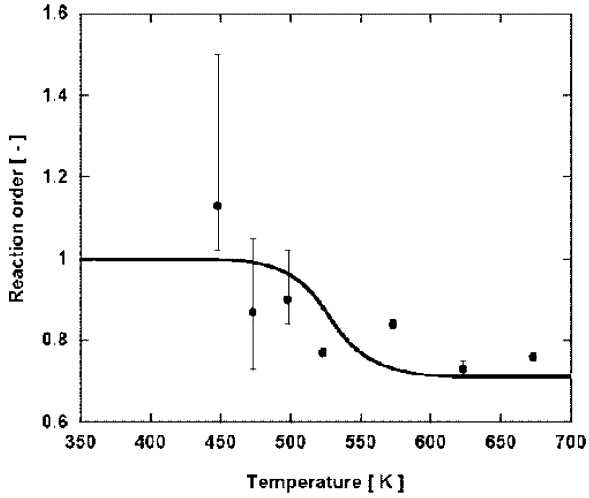

Figure 5. Reaction rate order for glucose in hydrothermal media as reported by Matsumura et al.[27] (Reprinted from ref 27. Copyright 2006 American Chemical Society.)

are empirical constants. A value of $n = 0.71$ was found to be the best fit to this data.

This less than first-order behavior has been reported recently in the literature for glucose reacting at hydrothermal conditions by Matsumura et al.[27] In their work, they observed that the rate order of glucose destruction under hydrothermal conditions drops below first order as the temperature is raised to or above about 225 °C; their results are shown in Figure 5. The value at 250 °C (523 K) reported by Matsumura is 0.77, in reasonable agreement with that measured in this study. Matsumura et al. employed a stainless steel tubular reactor with an inner diameter of 1.0 mm. They speculate that the drop in reaction rate order starting at temperatures around 250 °C may be due to a change in reaction mechanism as the reaction temperature is increased.

Glycine has been found to be essentially nonreactive at 250 °C and 10 MPa in the absence of glucose or a similarly reactive compound. Even at long residence times, the amount of glycine measured in the reactor effluent was found to be within error of the amount of glycine fed to the reactor when no glucose was present. A set of long residence time experiments was run in a continuous stirred tank reactor with residence times as long as 90 min. Even at these conditions, the amount of glycine destruction was not measurable; however, a small amount of

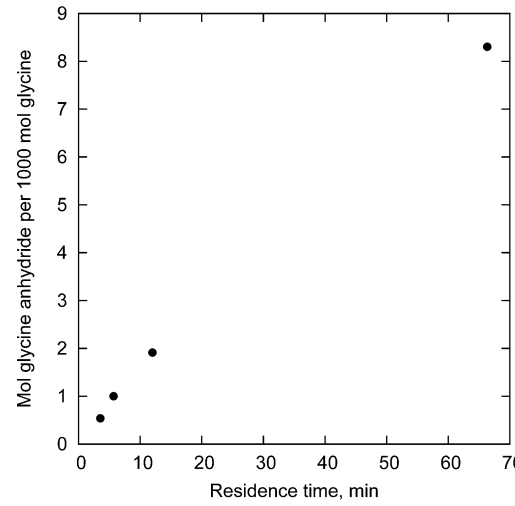

Figure 6. Reactor effluent concentration of glycine anhydride versus residence time for a feed mixture of 10.7 mmolal glycine at 250 °C and 5.5 MPa pressure.

glycine anhydride (a cyclical dimer of glycine) was detected in these long residence time reactions, as shown in Figure 6.

Glucose and Glycine Interactions. Numerous experiments conducted in this study confirm a strong interaction between glucose and glycine in hydrothermal media at 250 °C and 10 MPa. The presence of glucose or glycine has a large effect on the conversion kinetics of the other species. All experimental results are summarized in Table 1. Figure 7 shows the results of a set of experiments conducted at 250 °C, 10 MPa, 7.5 s residence time, and with an initial glycine concentration of 5 mmolal at the reactor inlet. In these experiments, the initial glucose concentration took on values between 0 and 10 mmolal. As can be seen, when no glucose was present, glycine was essentially nonreactive: the relative destruction was within the experimental error of zero. However, as the initial glucose concentration increased, the destruction of glycine continuously increased, up to values of about 32% destruction when the initial glucose concentration was 10 mmolal. The presence of glucose strongly affects the reactivity of glycine, providing kinetic evidence of a Maillard-type reaction between these two compounds.

The absorbance at 420 nm for this set of experiments is shown in Figure 8. Four-hundred twenty nanometers is a typical wavelength examined for products of the Maillard reaction;[28] neither glucose nor glycine absorbs at this wavelength. As can be seen, as the initial glucose concentration is increased from 0 to 10 mmolal, the absorbance rises monotonically, indicating the generation of colored compounds when the two compounds are reacted.

A similar set of experiments was conducted that kept the glucose feed at 5 mmolal and varied the glycine feed concentration between 0 and 10 mmolal. Reaction conditions for this experiment were again 250 °C, 10 MPa, and 7.5 s residence time. These results are summarized in Figure 9, which shows the relative destruction of glucose as a function of the initial glycine concentration. Glucose itself is reactive under hydrothermal conditions, and as can be seen in this figure, approximately 37% of the glucose feed is reacted with no glycine present. With the addition of glycine up to 10 mmolal, the amount of glucose destroyed raises to around 50%, although it does so in an asymptotic manner, rather than the nearly linear increase that was seen for the reverse set of experiments in Figure 7. The absorbance at 420 nm for this set of reactions is

Table 1. Summary of Runs[a]

$[Gly]_0$ (mmolal)	$[Glu]_0$ (mmolal)	res time (s)	temp (°C)	press. (MPa)	X_{gly}	X_{glu}	Abs_{420}	figures
4.97	0	7.5	250	10	0.02 ± 0.03		0.00059	7, 8
5.05	1.27	7.5	250	10	0.05 ± 0.03	0.44 ± 0.09	0.0051	7, 8
5.07	2.54	7.5	250	10	0.09 ± 0.03	0.46 ± 0.04	0.015	7, 8
5.04	5.06	7.5	250	10	0.15 ± 0.04	0.52 ± 0.02	0.049	7, 8
5.09	10.2	7.5	250	10	0.32 ± 0.03	0.56 ± 0.01	0.14	7, 8
0	5.08	7.5	250	10		0.37 ± 0.02	0.0019	9, 10
1.27	5.09	7.5	250	10	0.09 ± 0.06	0.48 ± 0.02	0.026	9, 10
2.55	5.06	7.5	250	10	0.16 ± 0.05	0.52 ± 0.02	0.038	9, 10
5.09	5.07	7.5	250	10	0.12 ± 0.03	0.51 ± 0.02	0.046	9, 10
10.2	5.09	7.5	250	10	0.11 ± 0.03	0.51 ± 0.02	0.058	9, 10
100	0	5.0	250	10	0.08 ± 0.04		0.0047	11−13
100	1.27	5.0	250	10	0.10 ± 0.04	NM[b]	0.042	11−13
100	2.51	5.0	250	10	0.09 ± 0.04	NM	NM	11−13
96.8	4.84	5.0	250	10	0.09 ± 0.04	NM	0.26	11−13
100	9.99	5.0	250	10	0.14 ± 0.03	NM	0.99	11−13
100	50.0	5.0	250	10	0.57 ± 0.02	NM	sat[c]	11−13
0	1.26	5.0	250	10	NM	0.49 ± 0.01	−0.000071	14, 15
1.25	1.25	5.0	250	10	NM	0.38 ± 0.01	0.0011	14, 15
2.51	1.25	5.0	250	10	NM	0.35 ± 0.01	0.0013	14, 15
5.03	1.26	5.0	250	10	NM	0.34 ± 0.01	0.0016	14, 15
10.16	1.27	5.0	250	10	NM	0.34 ± 0.03	0.0021	14, 15
0	1.25	5.0	250	10		0.50 ± 0.02	0.00061	16
0	2.50	5.0	250	10		0.41 ± 0.01	0.00087	16
0	5.00	5.0	250	10		0.34 ± 0.01	0.0014	16
0	10.0	5.0	250	10		0.28 ± 0.01	0.0026	16
1.25	0	5.0	250	10	0.00 ± 0.10		−0.00013	16
1.25	1.25	5.0	250	10	0.05 ± 0.05	0.40 ± 0.02	0.0012	16
1.25	2.50	5.0	250	10	0.08 ± 0.03	0.38 ± 0.01	0.0033	16
1.25	5.01	5.0	250	10	0.16 ± 0.03	0.36 ± 0.01	0.010	16
1.26	10.1	5.0	250	10	0.30 ± 0.02	0.35 ± 0.01	0.030	16
5.01	0	5.0	250	10	−0.01 ± 0.05		−0.000053	16
5.00	1.25	5.0	250	10	0.03 ± 0.05	0.35 ± 0.03	0.0017	16
5.00	2.50	5.0	250	10	0.05 ± 0.04	0.34 ± 0.03	0.0053	16
5.01	5.00	5.0	250	10	0.09 ± 0.04	0.35 ± 0.02	0.017	16
5.00	10.0	5.0	250	10	0.17 ± 0.04	0.37 ± 0.03	0.048	16
0	1.02	5.0	250	10		0.51 ± 0.03	NM	4
0	3.19	5.0	250	10		0.42 ± 0.02	NM	4
0	10.1	5.0	250	10		0.31 ± 0.02	NM	4
0	31.8	5.0	250	10		0.21 ± 0.01	NM	4
0	100	5.0	250	10		0.17 ± 0.01	NM	4

[a] X_{glu} and X_{gly} are the fractional molar conversions of glucose and glycine. Abs_{420} is the absorbance at 420 nm. [b] NM = not measured. [c] Sat = saturated detector.

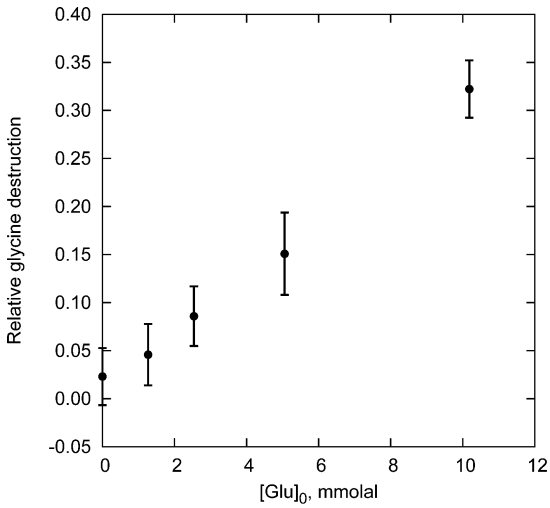

Figure 7. Destruction of glycine as a function of initial glucose concentration for experimental conditions of 250 °C, 10 MPa, 7.5 s, and an initial glycine concentration of 5 mmolal.

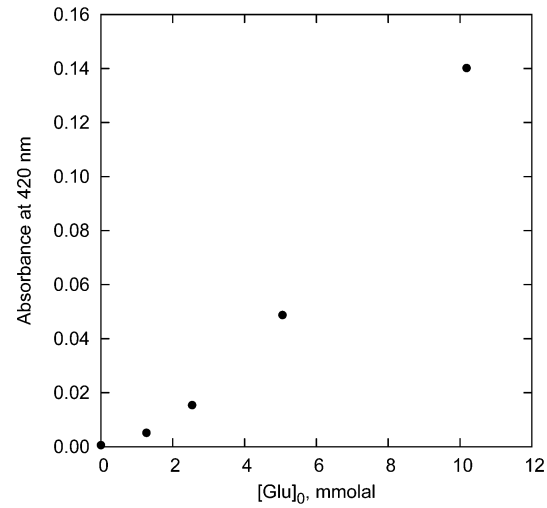

Figure 8. Absorbance at 420 nm as a function of initial glucose concentration, for experimental conditions of 250 °C, 10 MPa, 7.5 s, and an initial glycine concentration of 5 mmolal.

shown in Figure 10. Similar to the previous case, the absorbance at this wavelength increases as the initial concentration of glycine increases, indicating that the reaction between these two compounds produces colored species, consistent with the Maillard reaction.

At high feed concentrations, the reaction between glucose and glycine produces very visible results. Figure 11 visually shows the results of reacting 100 mmolal of glycine with 0−50 mmolal of glucose at 250 °C and 10 MPa for 5.0 s; as can be

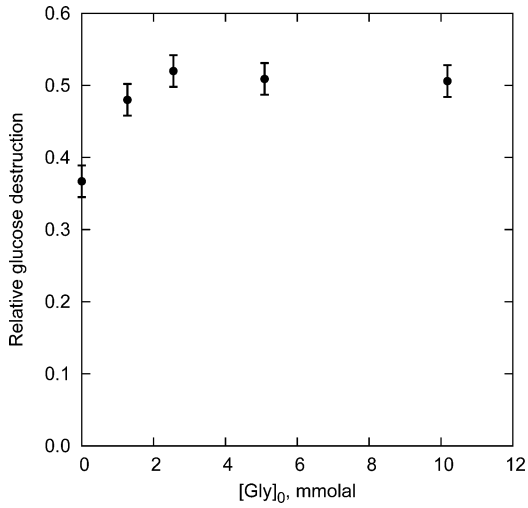

Figure 9. Destruction of glucose as a function of initial glycine concentration, for experimental conditions of 250 °C, 10 MPa, 7.5 s, and an initial glucose concentration of 5 mmolal.

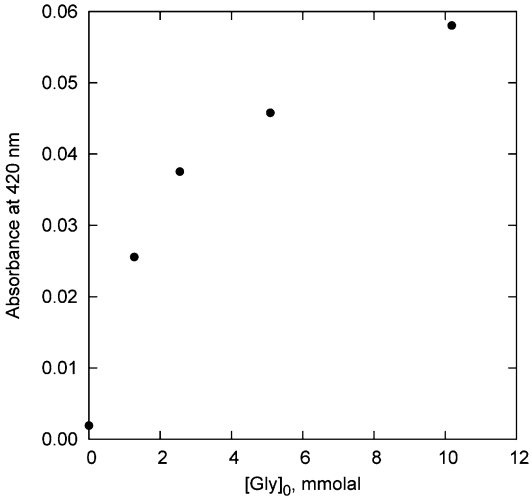

Figure 10. Absorbance at 420 nm as a function of initial glycine concentration, for experimental conditions of 250 °C, 10 MPa, 7.5 s, and an initial glucose concentration of 5 mmolal.

seen, the reactor effluent varied from nearly colorless when no glucose was added, to a rich brown color when glucose was present at 50 mmolal. Figure 12 shows the UV/vis absorbance spectra associated with these reactor effluents: the absorbance spectra confirm strong color generation throughout the visible range as the feed concentration of glucose is increased. This brown color generation is characteristic of a Maillard-type reaction. Qualitatively, a nutty odor is present during reactions of these two compounds, which is also characteristic of a Maillard-type reaction. At these high initial glycine concentrations, the amount of glycine destroyed continued to increase with increasing initial glucose concentration, reaching levels as high as 57% when glycine was fed at 100 mmolal and glucose was fed at 50 mmolal. This is shown in Figure 13.

The above results, and in particular Figures 7 and 9, show a strong interaction between glucose and glycine at hydrothermal conditions which is indicative of a Maillard-type reaction. To be sure, one would expect that if the Maillard reaction was occurring an increased presence of glycine would lead to an increased destruction of glucose, and vice versa. This is clearly the case in the two sets of experiments shown above. Indeed, in all hydrothermal experimental conditions tested, this effect was found to be universal with regards to the destruction of

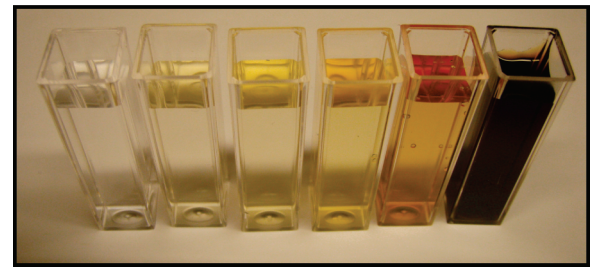

Figure 11. Reactor effluent samples from reactions of 100 mmolal glycine with, from left to right, 0, 1.3, 2.5, 5, 10, and 50 mmolal glucose.

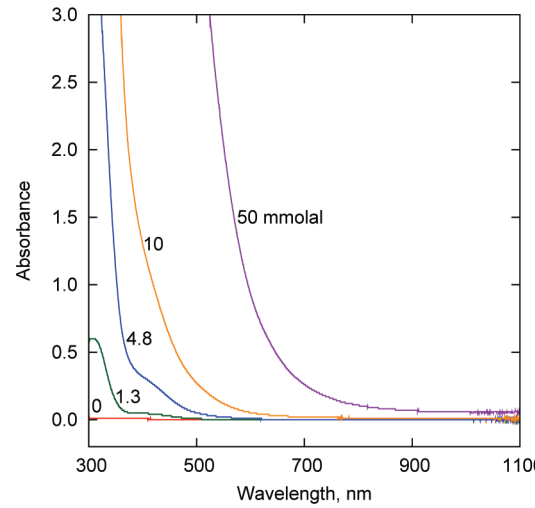

Figure 12. UV/vis absorbance spectra of reactor effluent from reactions of 100 mmolal glycine with varying amounts of glucose. The number on the curve corresponds to the concentration, in millimolal, of glucose in the reactor feed.

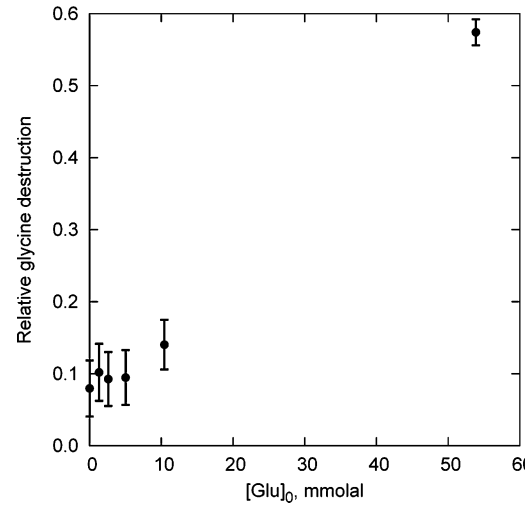

Figure 13. Destruction of 100 mmolal glycine as a function of initial glucose concentration, for experimental conditions of 250 °C, 10 MPa, and 5.0 s residence time.

glycine with a variable initial concentration of glucose. Per contra, this destruction pattern was not found to be universal for glucose destruction as a function of initial glycine loading: under certain conditions, a higher loading of glycine was found to have a protective effect on glucose.

This unexpected behavior is shown in Figure 14. This plot shows the relative destruction of an initial concentration of 1.25 mmolal glucose for a reaction at 250 °C, 10 MPa, and 5.0 s and with a variable initial glycine concentration. As can be seen,

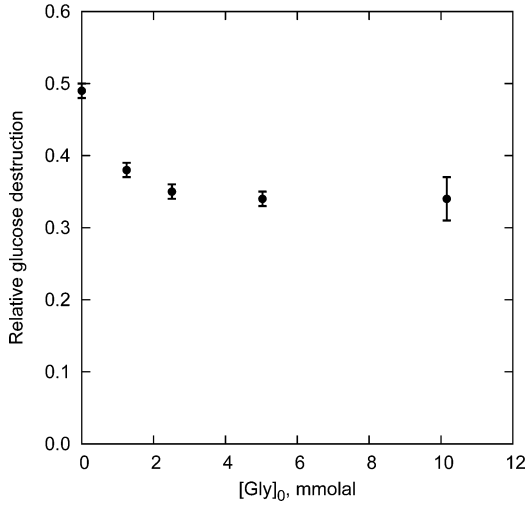

Figure 14. Destruction of 1.25 mmolal of glucose as a function of initial glycine concentration at 250 °C, 10 MPa, and 5.0 s.

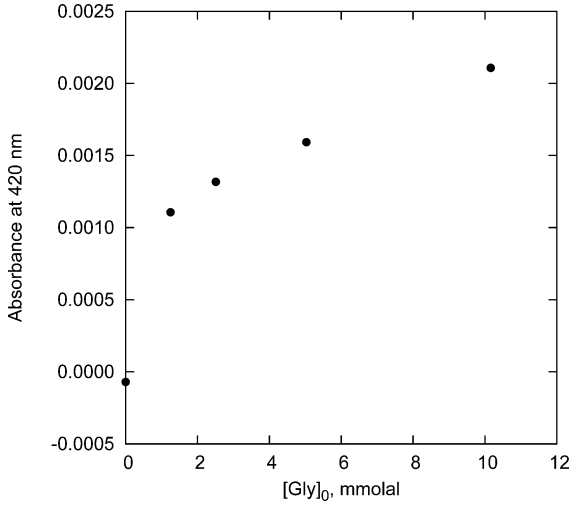

Figure 15. Absorbance at 420 nm as a function of initial glycine concentration, for experimental conditions of 250 °C, 10 MPa, 5.0 s, and an initial glucose concentration of 1.25 mmolal.

when no glycine was present, the destruction of glucose was ~49%. As the initial amount of glycine in the reactor was increased, the destruction of glucose dropped off to around 35%. However, as Figure 15 shows, the absorbance still increased with increasing glycine concentration, suggesting that any color-generating reactions still proceeded with greater effectiveness as the glycine concentration increased, even if the amount of glucose destroyed decreased under these conditions.

Figure 16 shows more detail in the region where the crossover between the expected and the unexpected behavior occurs. At relatively high initial glucose loadings of 10 mmolal, the destruction of glucose is seen to increase as the initial glycine concentration increases from 0 to 1.25 to 5 mmolal. On the left side of the chart, when glucose is at low initial concentrations, the amount of glucose destruction can be seen to *decrease* as the initial glycine concentration increases from 0 to 1.25 to 5 mmolal. The transition between these two types of behavior appears to occur at an initial glucose concentration of around 5 mmolal.

The "protective effect" has also been observed at lower temperatures. Ajandouz and Puigserver[29] found less glucose destruction in the presence of every amino acid they tested, in aqueous atmospheric-pressure reactions at 100 °C, pH 7.5, and

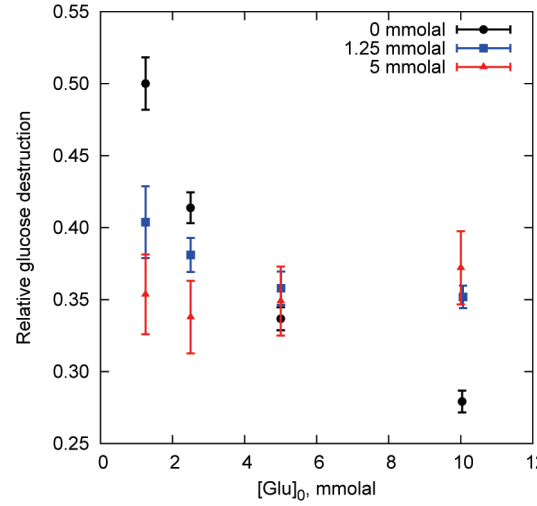

Figure 16. Glucose destruction for three different initial glycine loadings as a function of initial glucose concentration. In each case, reaction conditions were 250 °C, 10 MPa, and 5.0 s.

residence times of up to 120 min, as compared to aqueous glucose without amino acids. The amino acids they used were valine, leucine, isoleucine, tryptophan, phenylalanine, methionine, and lysine. Similarly and in a separate study, Ajandouz et al.[30] found that less fructose was destroyed in the presence of lysine than when it was reacted alone, for aqueous atmospheric-pressure reactions at 100 °C between pH values of 4.0 and 12.0.

More studies are necessary in order to understand the anomalous behavior observed under hydrothermal conditions. A number of possibilities could be envisioned for how glycine has this effect on glucose: the glycine could be quenching reactive intermediates that would have led to more glucose degradation, the glycine may be reversibly binding to the glucose itself and preventing its self-destruction, the glycine may be blocking sites on the reactor wall that would have otherwise catalyzed glucose destruction, or a Maillard-reaction product may be undertaking any of these roles. Additionally, since the protective effect is observed in the low-concentration region, it may be related to the less-than-first-order reaction kinetics observed for glucose alone. However, since the behavior was separately observed at much lower temperatures,[29,30] the behavior may be more universal. The Maillard reaction is well-known to produce species that exhibit antioxidant behavior;[31] it may be possible that these species quench reactive intermediates of the destruction of glucose. Glucose destruction by reactor-wall catalysis (and the blocking of these sites by glycine) is a possible cause; however, to fully explain these effects it would need to be caused by the nickel of the reactor in the present study, the stainless steel of the reactor employed by Matsumura et al.[27] and the glass walls employed by Ajandouz and colleagues.[29,30]

Related Compounds. One of the major products formed in the degradation of glucose under hydrothermal conditions is 5-hydroxymethylfurfural (HMF). HMF has been proposed as an industrial building block,[32] and as a precursor for carbohydrate-based fuels.[33] The production of HMF from the degradation of glucose was found to be hindered by the presence of glycine, indicating that the downstream degradation pathway was altered by the presence of glycine. Figure 17 shows the results of a set of experiments highlighting the production of HMF from an initial concentration of 5 mmolal glucose at 250 °C, 10 MPa, and 7.5 s residence time, with various starting concentrations of glycine present. The amount of HMF produced decreased

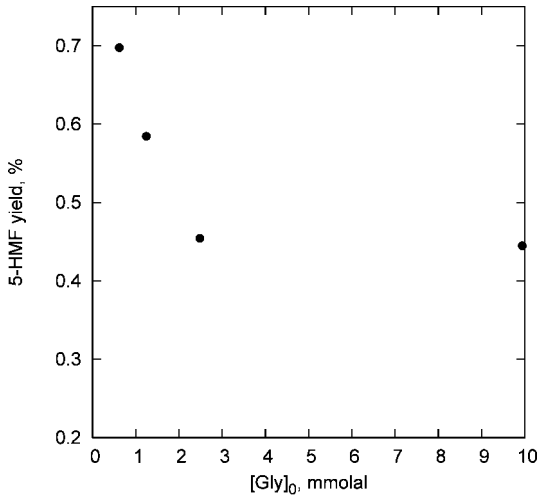

Figure 17. Yield of 5-hydroxymethylfurfural from 5 mmolal of glucose with varying amounts of glycine at 250 °C, 10 MPa, and 7.5 s residence time.

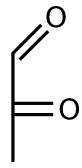

Figure 18. Chemical structure of pyruvic aldehyde.

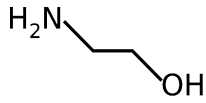

Figure 19. Chemical structure of ethanolamine.

from about 0.7% to about 0.45% as the initial glycine concentration increased from 0.6 to 10 mmolal. Under these conditions, an increase in initial glycine concentration results in increased destruction of glucose, as shown earlier in Figure 9. Although the increased glycine concentration leads to more glucose destruction, the destroyed glucose is being converted less selectively into HMF than would happen in the absence of glycine. This indicates that the presence of glycine is altering the downstream destruction path of glucose, and not just enhancing or reducing the degradation of glucose along the same pathway.

The degradation pathway of glucose in high-temperature, high-pressure water has been well mapped-out; see, for example, Figure 9 in the work of Peterson et al.[1] Examination of this hydrothermal reaction pathway of glucose shows that a number of compounds are produced which also have carbonyl groups; the carbonyl group is believed to be the functional group of glucose that is reactive in the initial step of the Maillard reaction (shown in Figure 1). It is logical to presume that these degradation compounds of glucose may also aid in the degradation of glycine. This is a somewhat unique aspect of the reaction at hydrothermal conditions, which would not be a concern at lower temperatures where glucose does not undergo single-molecule degradation reactions.

Among the compounds produced in the hydrothermal degradation of glucose, pyruvic aldehyde is a prime candidate to undergo a reaction with glycine since it has two functional carbonyl groups. The chemical structure of pyruvic aldehyde is shown in Figure 18. Figure 20 confirms that pyruvic aldehyde does have such an effect on the degradation of glycine. Shown

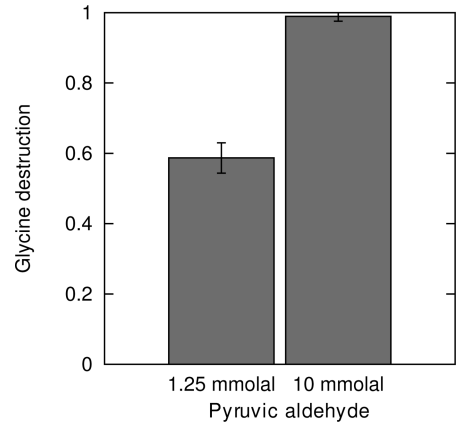

Figure 20. Destruction of 5 mmolal glycine with 1.25 mmolal and 10 mmolal of pyruvic aldehyde at 250 °C, 10 MPa, and 7.5 s residence time.

in this figure are the results of the reaction of 5 mmolal of glycine with 1.25 or 10 mmolal of pyruvic aldehyde at 250 °C, 10 MPa, and a residence time of 7.5 s. Under comparable conditions, glycine alone would essentially not react, and with the addition of glucose at 1.25 or 10 mmolal, the glucose destruction would be only on the order of 5 or 32%, as opposed to the 60−99% destruction seen with pyruvic aldehyde. This confirms that the reaction will be more complicated under hydrothermal conditions, as the degradation products of glucose can also participate in Maillard-type reactions, and appear to do so even more aggressively than glucose itself. Although absorbance data were not taken in these particular experiments, the reactor effluent had the rich brown color typical of the glucose−glycine experiments, as well as producing a similar nutty smell characteristic of Maillard-type reactions.

The faster reaction of pyruvic aldehyde with glycine, relative to the reaction of glucose with glycine, may be due to a number of factors. First, pyruvic aldehyde has two carbonyl functional groups, whereas glucose has only a single aldehyde group. Second, glucose may predominantly exist in a cyclic, nonreactive form, whereas pyruvic aldehyde has no such cyclic form. Third, pyruvic aldehyde is a smaller molecule and may exhibit less steric hindrance toward a reaction with glycine.

To test if other compounds presenting the primary amine functional group thought to be reactive on glycine can also degrade glucose, ethanolamine was used as a surrogate for glycine in a set of experiments. The chemical structure of ethanolamine is shown in Figure 19. The results of experiments comparing the destruction of glucose by glycine and ethanolamine are shown in Figure 21. These experiments were conducted at 250 °C and 10 MPa for 5.0 s and with an initial concentration of 10 mmolal of glucose, which was in the range noted earlier where glycine has the expected result of increasing the destruction of glucose. As can be seen, ethanolamine also reacts with glucose, and in a much more dramatic manner than glycine does.

Figure 22 shows the results of a similar set of experiments, but run with an initial concentration of glucose at 1.25 mmolal, which is in the range where the addition of glycine has the unexpected protective effect on the destruction of glucose. Reaction conditions were again 5.0 s at 250 °C and 10 MPa. As can be seen, glycine exhibits the protective effect on glucose under these conditions, but the presence of ethanolamine at both concentrations tested, 1.25 and 5 mmolal, leads to significantly more destruction of glucose than in the case when no amine-presenting group was present. However, comparing the destruc-

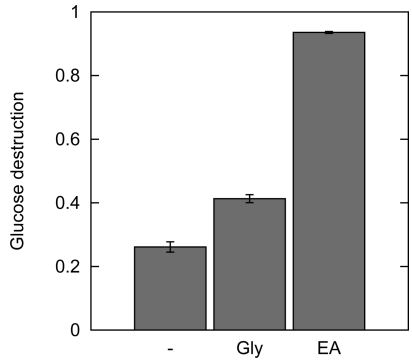

Figure 21. Destruction of 10 mmolal of glucose by 5 mmolal of glycine (Gly), by 5 mmolal of ethanolamine (EA), and in the absence of either compound (−) at 250 °C, 10 MPa, and 5.0 s residence time.

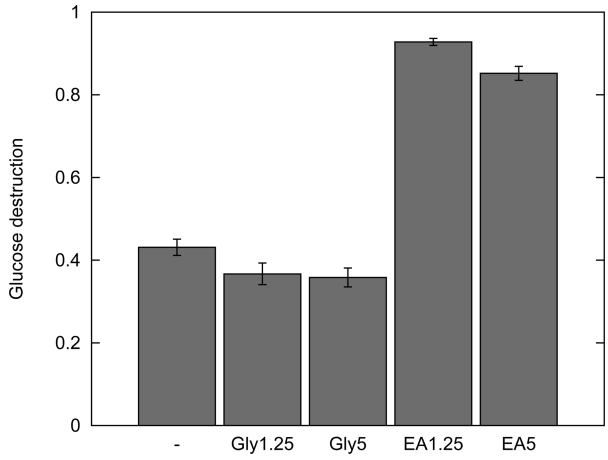

Figure 22. Destruction of 1.25 mmolal of glucose alone (−), by 1.25 mmolal of glycine (Gly1.25), by 5 mmolal of glycine (Gly5), by 1.25 mmolal of ethanolamine (EA1.25), and by 5 mmolal of ethanolamine (EA5) at 250 °C, 10 MPa, and 5.0 s residence time.

tion of glucose by 1.25 and 5 mmolal of ethanolamine, it is seen that the higher concentration of ethanolamine results in *less* destruction of glucose than the lower concentration of ethanolamine, which is the same trend seen for glycine. Thus, an aspect of the unexpected protective effect was observed with ethanolamine in addition to glycine.

4. Conclusions

(1) A strong interaction has been demonstrated between glucose and glycine in water at 250 °C and 10 MPa. This interaction is demonstrated both in changes in reaction kinetics and in the qualitative observations of the development of brown colors and characteristic odors associated with the Maillard reaction.

(2) The destruction of glycine in the reactor was correlated with the glucose concentration fed to the reactor, and a greater initial concentration of glucose always led to more destruction of glycine.

(3) The destruction of glucose in the reactor was affected by the glycine concentration fed to the reactor, but the glucose destruction could either be increased or decreased by the presence of glycine. Generally, glycine exhibited a "protective" effect on glucose when the initial glucose concentration was low (<5 mmolal) and the residence time was short (5.0 s, rather than 7.5 s).

(4) Glucose was observed to exhibit less-than first-order kinetics under these conditions (in the absence of glycine), confirming earlier reports by Matsumura et al.[27] This may be partially responsible for the unexpected protective effect that glycine has on glucose at certain conditions. Glycine was found to be essentially nonreactive by itself, with only a small amount of glycine anhydride (a dimer of glycine) produced at very long residence times.

(5) Unique to the hydrothermal environment, degradation products of glucose may also participate in the first step of the Maillard reaction. This was demonstrated by the reaction of pyruvic aldehyde, a glucose degradation product, with glycine. Pyruvic aldehyde was observed to react more strongly with glycine than glucose did, with the same qualitative effects of a brown color and odor production.

(6) Reactions of surrogate compounds for glucose and glycine also exhibited similar effects, implying that the nucleophilic attack of the primary amine group of glycine on glucose is the active reaction at hydrothermal conditions. As a surrogate for glycine, ethanolamine was found to react strongly with glucose, and to partially reproduce the protective effect on glucose that glycine had under certain conditions. The demonstration of the reactivity of pyruvic aldehyde with glycine showed that the carbonyl functional group was likely the functional part of glucose.

The evidence produced in this study indicates that a Maillard-type reaction readily occurs under conditions of significance to hydrothermal biomass processing into biofuels and chemicals. This will undoubtedly prove to be of significance in the further development of these processes, as processes that contain significant quantities of proteins or amino acids can be expected to undertake uniquely different reaction pathways. While this study highlighted the reactivity of a simple sugar and amino acid, in hydrothermal media both peptide bonds and glycosidic linkages undergo hydrolysis, therefore, polymeric forms of these chemicals would also be expected to be reactive, including oligosaccharides, polysaccharides (starch, cellulose, hemicellulose, glycogen), peptides, and proteins. This behavior explains the observations in the process trials undertaken by Changing World Technologies and by the Forschungszentrum Karlsruhe. As hydrothermal technologies are further developed to take a wider range of feedstocks, including waste products and protein-containing feedstocks such as algae or microbes, attention will need to be paid to the effects of the levels of protein in the feeds.

Acknowledgment

We thank Terry Adams and Brian Appel of Changing World Technologies, Inc., for discussions and suggestions in this study. We particularly thank Sam Maurer and Drew Cameron at MIT for research assistance and insights in this project. We acknowledge and appreciate financial support from the Martin Family Foundation, the Paul Scherrer Institut, and the Society for Energy and Environmental Research (through U.S. Department of Energy (DOE) award DE-FG36-04GO14268). Support by the DOE does not constitute endorsement by the DOE of the views expressed in this article.

Literature Cited

(1) Peterson, A. A.; Vogel, F.; Lachance, R. P.; Fröling, M.; Antal, M. J., Jr.; Tester, J. W. *Energy Environ. Sci.* **2008**, *1*, 32–65.

(2) Waldner, M. Catalytic hydrothermal gasification of biomass for the production of synthetic natural gas, Thesis, ETH Zürich, 2007; No. 17100; http://e-collection.ethbib.ethz.ch/view/eth:29520.

(3) Vogel, F.; Waldner, M.; Rouff, A.; Rabe, S. *Green Chem.* **2007**, *9*, 616–619.

(4) Waldner, M.; Vogel, F. *Ind. Eng. Chem. Res.* **2005**, *44*, 4543–4551.

(5) Elliott, D.; Neuenschwander, G.; Hart, T.; Butner, R.; Zacher, A.; Engelhard, M.; Young, J.; McCready, D. *Ind. Eng. Chem. Res.* **2004**, *43*, 1999–2004.

(6) Goudriaan, F.; van de Beld, B.; Boerefijn, F. R.; Bos, G. M.; Naber, J. E.; van der Wal, S.; Zeevalkink, J. A. Thermal efficiency of the HTU(R) process for biomass liquefaction. In *Progress in Thermochemical Biomass Conversion*; Bridgwater, A. V., Ed.; Blackwell Science Ltd., 2001.

(7) Fröling, M.; Peterson, A.; Tester, J. Hydrothermal processing in biorefineries - a case study of the environmental performance. In *7th World Congress of Chemical Engineering*, Glasgow, Scotland, July 10−14 2005.

(8) Svanström, M.; Patrick, T. N.; Fröling, M.; Peterson, A. A.; Tester, J. W. *J. Adv. Oxidation Technol.* **2007**, *10*, 177–185.

(9) Peterson, A. A.; Vontobel, P.; Vogel, F.; Tester, J. W. *J. Supercrit. Fluids* **2008**, *43*, 490–499.

(10) Peterson, A. A.; Vontobel, P.; Vogel, F.; Tester, J. W. *J. Supercrit. Fluids* **2009**, *49*, 71–78.

(11) Hodes, M.; Marrone, P.; Hong, G.; Smith, K.; Tester, J. *J. Supercrit. Fluids* **2004**, *29*, 265–288.

(12) Marrone, P.; Hodes, M.; Smith, K.; Tester, J. *The Journal of Supercritical Fluids* **2004**, *29*, 289–312.

(13) Hodge, J. *J. Agric. Food Chem.* **1953**, *1*, 928–943.

(14) Martins, S. Unravelling the Maillard reaction network by multiresponse kinetic modelling, Thesis, Wageningen University, The Netherlands, 2003.

(15) Monnier, V. M.; Sell, D. R.; Wu, X.; Rutter, K. *Int. Congress Ser.* **2002**, *1245*, 9–19.

(16) Adams, T., unpublished data.

(17) Kruse, A.; Krupka, A.; Schwarzkopf, V.; Gamard, C.; Henningsen, T. *Ind. Eng. Chem. Res.* **2005**, *44*, 3013–3020.

(18) Kruse, A.; Maniam, P.; Spieler, F. *Ind. Eng. Chem. Res.* **2007**, *46*, 87–96.

(19) Inoue, S.; Noguchi, M.; Hanaoka, T.; Minowa, T. *J. Chem. Eng. Jpn.* **2004**, *37*, 915–919.

(20) Minowa, T.; Inoue, S.; Hanaoka, T.; Matsumura, Y. *Nihon Enerugi Gakkaishi/J. Jpn. Inst. Energy* **2004**, *83*, 794–798.

(21) Hill, V. M.; Isaacs, N. S.; Ledward, D. A.; Ames, J. M. *J. Agric. Food Chem.* **1999**, *47*, 3675–3681.

(22) Moreno, F. J.; Molina, E.; Olano, A.; Lopez-Fandino, R. *J. Agric. Food Chem.* **2003**, *51*, 394–400.

(23) Bristow, M.; Isaacs, N. *J. Chem. Soc.—Perkin Trans. 2* **1999**, 2213–2218.

(24) Peterson, A. Biomass Reforming Processes in Hydrothermal Media, Thesis, Massachusetts Institute of Technology, 2009.

(25) Phenix, B.; DiNaro, J.; Tester, J.; Howard, J.; Smith, K. *Ind. Eng. Chem. Res.* **2002**, *41*, 624–631.

(26) Marrone, P. Hydrolysis and oxidation of model organic compounds in sub- and supercritical water: Reactor design, kinetics measurements, and modeling, Thesis, Massachusetts Institute of Technology, 1998; http://hdl.handle.net/1721.1/9964.

(27) Matsumura, Y.; Yanachi, S.; Yoshida, T. *Ind. Eng. Chem. Res.* **2006**, *45*, 1875–1879.

(28) Morales, F. J.; Jiménez-Pérez, S. *Food Chem.* **2001**, *72*, 119–125.

(29) Ajandouz, E. H.; Puigserver, A. *J. Agric. Food Chem.* **1999**, *47*, 1786–1793.

(30) Ajandouz, E.; Tchiakpe, L.; Ore, F. D.; Benajiba, A.; Puigserver, A. *J. Food Sci.* **2001**, *66*, 926–931.

(31) Pokorný, J. *Trends Food Sci. Technol.* **1991**, *2*, 223–227.

(32) Kunz, M. Hydroxymethylfurfural - a possible basic chemical for industrial intermediates. In *Studies in Plant Science, Vol 3 Inulin and inulin-containing crops*; Fuchs, A., Ed.; Elsevier: Amsterdam, NY, 1993.

(33) Roman-Leshkov, Y.; Barrett, C. J.; Liu, Z. Y.; Dumesic, J. A. *Nature* **2007**, *447*, 982–985.

Received for review September 20, 2009
Revised manuscript received January 7, 2010
Accepted January 13, 2010

IE9014809